ARCHIVES
of
FOUNDRY ENGINEERING

ISSN (2299-2944)
Volume 2026
Issue 1/2026

77 – 83

8/1

10.24425/afe.2026.157971

Published quarterly as the organ of the Foundry Commission of the Polish Academy of Sciences

# Design of Methodology for Static and Dynamic Tests of Hybrid Castings

**M. Bruna [a], M. Medňanský [a,*], M. Kuriš [b], J. Španielka [b]**

[a] Faculty of Mechanical Engineering, Department of Technological Engineering, University of Zilina, Univerzitná 8215/1, 010 26 Žilina, Slovakia

[b] Institute of Materials and Machine Mechanics, Slovak Academy of Sciences, Inoval - Innovation center, Priemyselná 525 Ladomerská Vieska, 965 01 Žiar nad Hronom, Slovakia

* Corresponding author: e-mail: martin.mednansky@fstroj.uniza.sk

Received 11.07.25; accepted in revised form 13.11.25; available online 30.03.2026

## Abstract

This paper investigates hybrid aluminum castings produced by the overcasting method, targeting lightweight solutions for the engineering industry. The novelty of this work lies in the systematic evaluation of how foaming pressure parameters and subsequent core surface treatments influence the final mechanical properties of these complex components. The principle of this innovative technique is to overcast a porous cellular core, which is created by foaming a molten aluminum alloy. Porous cores were fabricated using various foaming pressures, and their influence on mechanical performance was assessed through uniaxial compression and impact tests. The results demonstrate that controlled foaming pressures, specifically starting pressures of 0.1–0.2 MPa and stabilizing pressures of 0.05 MPa and 0.101 MPa, yield porous cores with the most consistent and highest compressive strength. Crucially, the integrity of the final hybrid casting is highly dependent on the surface treatment of the core prior to overcasting. X-ray tomography revealed that treating the core with 10% $H_3PO_4$ acid effectively prevents molten metal penetration, resulting in a compressive strength three times higher than that of untreated or improperly treated castings. Furthermore, impact testing showed that the porous cores exhibit an average impact toughness 3.4 times higher than solid specimens of the same dimensions, highlighting their superior energy absorption capabilities.

**Keywords:** Hybrid castings, Aluminium foam, Overcasting technology, Mechanical testing

## 1. Introduction

To meet carbon neutrality requirements, the automotive industry is actively seeking lightweighting solutions. While methods like high-pressure die casting or additive manufacturing are utilized [1,2], they can be energy-intensive and not always economically viable [3,4]. This paper presents an alternative technology: producing hybrid castings by using a low-density core made of metal foam through an overcasting process.

Overcasting is a manufacturing technology where a liquid metal is brought into contact with a solid metal, creating a diffusion reaction zone between them [5,6]. A significant challenge in joining aluminum-aluminum alloys is the presence of the stable, high-melting-point (2072 °C) aluminum oxide ($Al_2O_3$) layer on the surface, which limits wettability. This problem was previously addressed by replacing the $Al_2O_3$ layer with a low-melting-point zinc coating [6].

This paper considers metal foams as the solid-state material for the overcasting process. These are materials with a cellular structure, where pores make up more than 70 % of the volume. Cellular structures are typically categorized into open-pore (interconnected) and closed-pore structures [7]. Metal foams are noted for their low specific weight and high energy absorption capabilities. While open-pore foams are suitable for applications like heat exchangers [8,9], closed-pore foams are primarily used to

absorb impact energy, also recent reviews highlight that closed-cell aluminum foams combine low density with excellent energy absorption and stiffness, making them suitable for structural and impact-mitigation components [10, 11].

In energy absorbing applications, the compressive strength of metal foam is particularly important. The compressive stress-strain curve of metal foam generally consists of three distinct regions: an initial linear-elastic deformation, a long plastic deformation plateau at near-constant stress, and finally a compaction region where stress rapidly increases [11-13].

The cores themselves are produced via a powder metallurgy route, where a precursor containing a foaming agent (TiH2) is heated, causing the agent to decompose and expand the material into a closed-pore structure. While the properties of aluminum foams are well-documented, their application as cores in hybrid castings presents unique challenges, particularly regarding the interface integrity and mechanical response of the final composite part [13-15].

The primary objective of this research was to systematically assess the influence of key manufacturing parameters on the mechanical properties of two distinct elements: porous cores and final hybrid castings. The investigation was focused on two specific areas. First, the effect of applied foaming pressure on the compressive strength and consistency of the cores was studied. Second, the impact of different core surface treatments on the structural integrity and performance of the overcast component was evaluated. The novelty of this work lies in establishing a direct correlation between these processing parameters and the final mechanical behavior, providing a methodological framework for optimizing the production of lightweight, high-performance hybrid castings.

## 2. Materials and methods

The number of samples tested in each group was three for compression and four for impact tests.

The foamable precursor material was fabricated using a powder metallurgy (PM) route, as illustrated in Figure 1. The input material consisted of a powder mixture of pure Al (89.2 wt. %), Si as the primary alloying element (10 wt. %), and $TiH_2$ as the foaming agent (0.8 wt. %).

Following thorough mixing, the powders were compacted into billets (Ø200 mm x 1000 mm) by cold isostatic pressing (CIP) at a pressure of 150 MPa. These billets were subsequently extruded into a continuous, semi-finished strip with a 50 × 4 mm cross-section. This precursor is designed to expand into a closed-cell foam when heated, as the $TiH_2$ foaming agent decomposes and releases hydrogen gas [7,10].

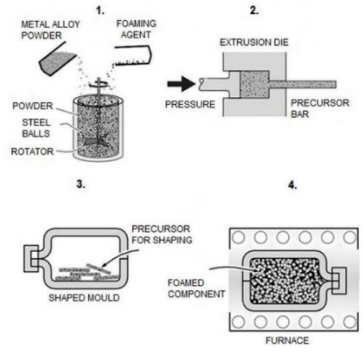


Fig. 1. Process of the PM route of foam manufacturing [10]

The foaming process was carried out in an furnace with a controlled temperature and a protective atmosphere pressure. The mold, which determines the shape of the foamed material, is an extruded graphite block milled into the desired shape. The cores intended for overcasting have a cylindrical geometry with protrusions designed to position the core within the mold and improve the mechanical bond. Cores for the impact bending test have a prismatic shape. To prevent degradation of the graphite at high temperatures, the furnace chamber is filled with a protective nitrogen (N2) atmosphere. The dimensions are shown in Figure 2.

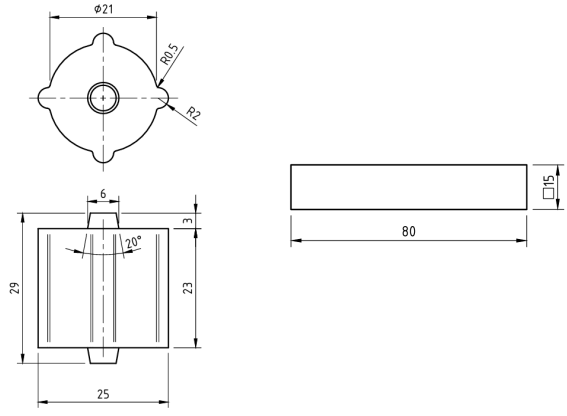


a) b)

Fig. 2. Porous cores dimensions. a) cylindrical, b) prismatic

The shaped cylindrical and prismatic foam cores were foamed at various initial and stabilizing pressures, according to Tables 1 and 2.

Table 1.
Pressure regimes for foaming of the cylindrical porous cores

| Variant # | Starting pressure [MPa] | Stabilising pressure [MPa] |
|---|---|---|
| **V1** | 0.101 | 0.005 |
| **V2** | 0.15 ÷ 0.2 | 0.15 |
| **V3** | 0.1 ÷ 0.2 | 0.1 |
| **V4** | 0.1 ÷ 0.2 | 0.15 |
| **V5** | 0.1 ÷ 0.2 | 0.05 |
| **V6** | 0.1 ÷ 0.2 | 0.101 |
| **V7** | 0.1 ÷ 0.3 | 0.15 |

Table 2.
Pressure regimes for foaming of the prismatic porous cores

| Variant # | Starting pressure [MPa] | Stabilising pressure [MPa] |
|---|---|---|
| **VP1 and VP2** | 0.3 | 0.125 MPa |
| **VP3 and VP4** | 0.37 | 0.2 MPa |

Only specific combinations of core variants and surface treatments were selected for the overcasting process. Based on the results from the previous experimental step, three variants exhibiting the desired properties were chosen. These cores were surface-treated using hydrofluoric (HF) acid and phosphoric ($H_3PO_4$) acid. The procedure for this surface treatment is summarized in Table 3.

Table 3.
Surface treatment of the porous cores for overcasting

| Step | N | F | P1 | P4 |
|---|---|---|---|---|
| **1** | Degreasing by rubbing each side with isopropyl alcohol | | | |
| **2** | Drying | Drying | Drying | Drying |
| **3** | x | Bathing each side in HF 0.5% for 20 s | Bathing each side in $H_3PO_4$ 10% for 1:30 min at 50 °C | Bathing each side in $H_3PO_4$ 10% for 4:00 min at 50 °C |
| **4** | x | Drying | Drying | Drying |
| **5** | x | Rubbing each side with 99.5% isopropyl alcohol | | |
| **4** | x | Drying | Drying | Drying |
| **6** | Preheating in electric resistance furnace at 150 ± 10 °C for 15 minutes | | | |

The AlSi7Mg0.3 alloy was selected for overcasting the foam cores using gravity casting technology. The chemical composition of this alloy is summarized in Table 4. The material was melted in an electric resistance furnace, and the pouring temperature was 760 ± 10 °C.

Table 4.
Chemical composition of AlSi7Mg0.3 [wt. %]

| Si | Mg | Fe | Mn | Ti |
|---|---|---|---|---|
| 6.5 – 7.5 | 0.25 – 0.45 | max. 0.19 | max. 0.1 | max. 0.25 |
| **Cu** | **Zn** | **Others** | | **Al** |
| max. 0.05 | max. 0.07 | each 0.03; total 0.1 | | balanced |

The second-generation molds were made from a mixture of silica foundry sand and a phenol-formaldehyde resin, curable with $CO_2$ (Figure 3). The mold cavity was milled into the cured block. The molds were preheated to a temperature of 150 ± 10 °C for 15–20 minutes.

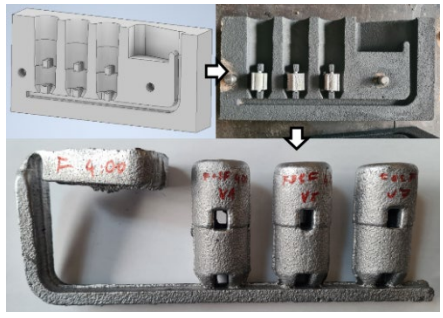

Fig. 3. Overcasting process

Using the same gravity casting method, solid prismatic reference samples of the AlSi7Mg0.3 alloy were also created in the second-generation molds, intended for the impact bending test.

## 2.1. Compression testing of the porous cores and hybrid castings

The cylindrical foam cores were subjected to a static compression test. Their end surfaces were prepared by removing the geometric protrusions, as depicted in Figure 4a). Three samples from each of the seven variants (V1 to V7), which differed according to the foaming parameters in Table 1, were tested. The test was performed on a universal testing machine with a 20 kN maximum load capacity at a rate of 1 mm·min$^{-1}$. The termination condition for the measurement was set to a crosshead displacement of $\Delta h$ = 18 mm, corresponding to a material strain of $\varepsilon$ = 0.78 %. The compressive force acting on the sample was recorded during the test.

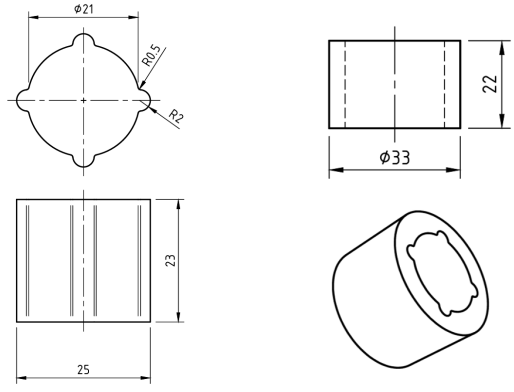


a) b)

Fig. 4. Specimen dimensions for compression testing. a) foam core, b) hybrid casting

Prior to the static compression test, the hybrid castings were analyzed using a Nikon XT H225 ST computed tomography (CT) scanner to determine the areal porosity of the casting. The computed tomography (CT) scans were conducted using an X-ray tube voltage of 220 kV and a tube current of 68 µA, parameters selected to provide sufficient beam energy for optimal sample penetration while maintaining image contrast. The imaging setup

achieved an effective pixel resolution of 25 µm, enabling high-resolution reconstruction suitable for detailed morphological assessment. A total of 720 projections were acquired, with 4 frames per projection to enhance image quality through frame averaging and noise reduction. Furthermore, a 0.1 mm copper (Cu) filter was employed to attenuate low-energy photons, thereby minimizing beam hardening artifacts and improving the overall spectral uniformity of the X-ray beam.

The static compression test was performed on the "Overcast" hybrid castings with dimensions according to Figure 4b). Due to the solid metal shell, it was necessary to use a testing machine with a higher maximum force capacity. For the compression test of the hybrid castings, the termination condition was set to a measured compressive force of 190 kN. The samples were loaded at a rate of 1 mm·min$^{-1}$.

## 2.2. Impact bending test

Four prismatic foam samples and two solid material samples, with the geometry shown in Figure 2b), were subjected to a dynamic impact bending test. The samples were unnotched, as they are a low-strength material. The impact bending test was performed on a Charpy pendulum impact tester with a maximum developed energy of 300 J. After the absorbed energy was measured, the impact toughness was calculated according to the following formulas:

$$KC0 = \frac{K}{S}\ [J.cm^{-2}] \tag{1}$$

$$\rho_{relat} = \frac{m_P}{m_S} = \frac{\rho_P}{\rho_S} = \frac{S_P}{S_S}[-] \tag{2}$$

$$S_P = S_S \cdot \rho_{relat} = S_S \cdot \frac{m_P}{m_S}\ [cm^2] \tag{3}$$

$$KC0 = \frac{K}{S_S \cdot \frac{m_P}{m_S}}\ [J.cm^{-2}] \tag{4}$$

Where:

- KC0 is the impact toughness [J·cm$^{-2}$],
- K is the absorbed energy [J],
- $S_0$ is the cross-sectional area of the unnotched sample [cm$^2$],
- $\rho_{relat}$ is the relative density [-], determined by the ratio of the mass, density, or cross-section of the measured sample to a solid sample of the same volume,
- $S_P$ is the cross-sectional area of the porous sample, determined from relation (2) [cm$^2$],
- $m_P$ is the measured mass of the porous sample [g],
- $m_S$ is the mass of a solid sample of the same dimensions [g], which can be considered a constant of 43 g.

Note: All impact tests were conducted at ambient temperature (22 ± 1 °C).

# 3. Results and discussion

The static uniaxial compression test, performed on 21 porous core samples, revealed mechanical behaviors consistent with established literature on closed-cell metallic foams. The compression curves for all variants, as representatively shown for V5 in Figure 5, exhibit three characteristic regions: an initial linear-elastic response, a prolonged deformation plateau, and a final stage of rapid densification. This three-stage behavior is in strong agreement with foundational models, where the elastic region corresponds to cell wall bending, the plateau is governed by the progressive collapse of pores via plastic hinging and buckling, and densification occurs as opposing cell walls crush against each other.

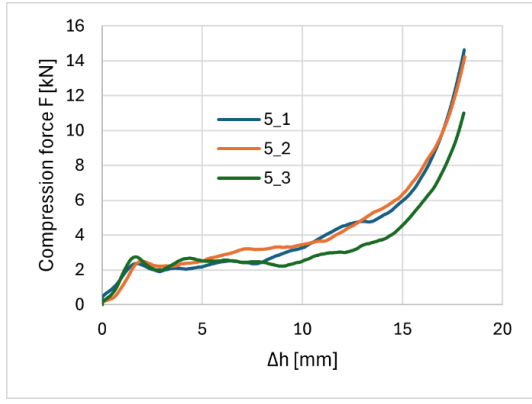


Fig. 5. Static uniaxial compression testing of the V5 porous cores. Interval Δh = (0 – 18) mm

The maximum compressive forces achieved for each sample are compared over a displacement interval of (0–18) mm. To determine the "level force" (i.e., the force at which stabilization occurs with increasing displacement), only the interval of Δh = (0–5) mm is analyzed (Figure 6). The value of the "level force" was identified as the maximum force within this specific interval.

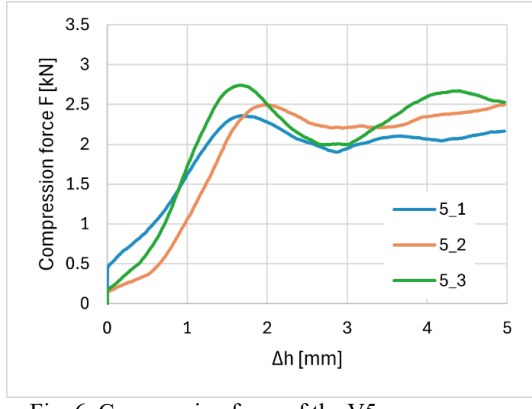


Fig. 6. Compression force of the V5 porous cores. Interval Δh = (0 – 5) mm

The maximum forces determined from these measurements, as well as the measured "level forces," are summarized in the graphs

in Figures 7 and 8. The values were arithmetically averaged, and the standard deviation was determined.

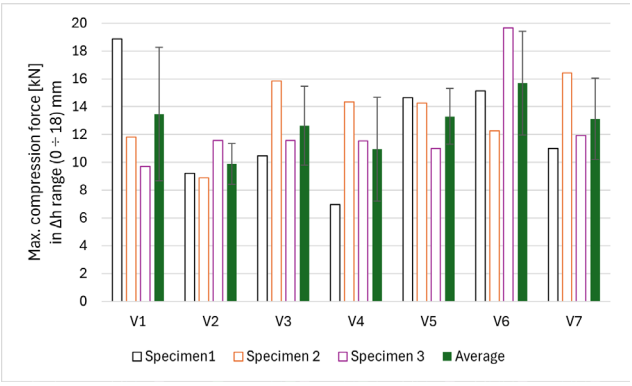


Fig. 7. Maximum compression force after 18 mm of deformation

From the measurement results, a high variability of results can be observed within some of the variants. At this stage of the research, repeatability of the results is a desired property. A critical finding of this study is the profound impact of foaming pressure on the repeatability of mechanical properties, a key factor for any industrial application. The results summarized in Figure 7 and 8 clearly show that variant V1, foamed under uncontrolled atmospheric pressure, exhibited the highest standard deviation in both maximum compressive force and level force. This high variability can be attributed to the uncontrolled growth of pores, leading to an inconsistent and non-uniform cellular structure, a phenomenon widely recognized to compromise the reliability of foam properties. In contrast, the application of a controlled stabilizing pressure significantly influenced the foam's structural integrity. Variants V2 and V4, which utilized a relatively high stabilizing pressure of 0.15 MPa, yielded cores with lower average compressive strength. This outcome is likely due to pore coarsening, where higher internal gas pressure promotes the formation of larger, non-uniform pores with thinner cell walls. Such structures are mechanically weaker and less capable of distributing load effectively. The most favorable results were achieved with variants V5 and V6, which used moderate stabilizing pressures (0.05 MPa and 0.101 MPa). This pressure range appears to strike an optimal balance, facilitating controlled foam expansion while preventing excessive pore growth, thus resulting in a finer and more uniform cell structure with enhanced strength and, crucially, lower variability. These findings underscore the necessity of precise pressure control during the foaming process to produce cores with reliable and predictable mechanical performance.

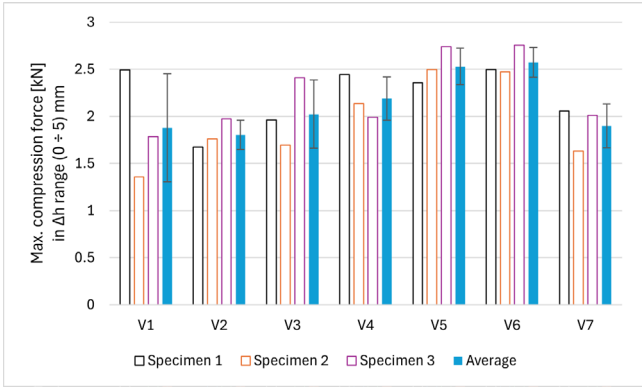


Fig. 8. Level force measured in Δh = (0 – 5) mm

After taking these results into account, samples from variants V1 (as the reference), V5, and V7 were selected for overcasting with liquid metal. The course of the static compression test for the hybrid casting samples is summarized in Figure 9. The variants are color-coded according to the surface treatment applied to the core.

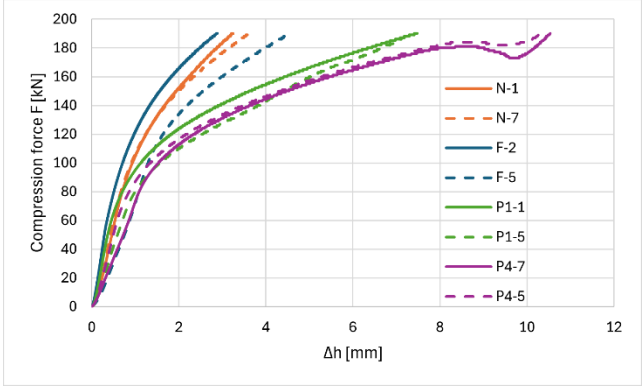


Fig. 9. Static uniaxial compression testing of the hybrid castings

Hybrid castings whose porous cores were not surface-treated (N-x variants) exhibit the highest strength with the lowest deformation. In contrast, the hybrid castings subjected to the greatest deformation were those, where the core was surface-treated with 10% $H_3PO_4$. This phenomenon is explained in Figure 10, which shows computed tomography (CT) images of the hybrid castings' cross-sections. In the case of the non-surface-treated variant, significant penetration of the molten metal into the porous core can be observed. The melt breached the outer skin of the porous material and flowed into the pore cavities. Gas from the pores was forced out into the solidifying metal surrounding the core, which resulted in increased porosity in the solid shell of the sample. A similar result can be observed when a 0.5% HF treatment was used on the surface of the porous core. The areal porosity values in cross-sections through the sample's center in various planes are recorded in Table 5.

The most significant outcome of this investigation is the success of the phosphoric acid ($H_3PO_4$) treatment (P1 and P4 variants). This process is known to create a more stable and continuous phosphate conversion coating on the aluminum surface. This layer acts as a robust physical barrier that effectively prevents

melt infiltration, even at high casting temperatures. The CT scans confirm that the porous structure of the core was fully preserved. This allowed the hybrid casting to function as designed: a strong, solid shell encasing a lightweight, deformable core. Consequently, these castings exhibited vastly superior ductility, withstanding large deformations and achieving a compressive strength approximately three times higher than the infiltrated samples before failure. This demonstrates that a properly formed phosphate barrier is essential for manufacturing structurally sound hybrid castings using this technology.

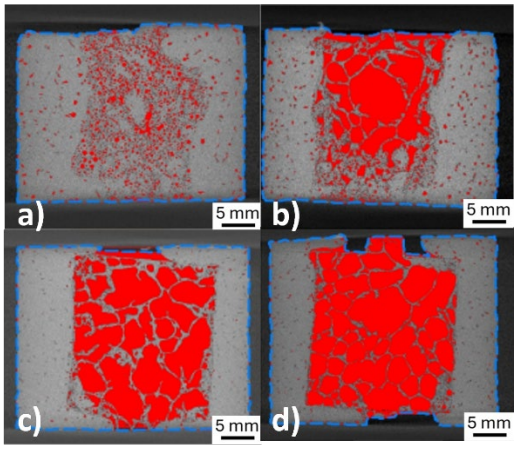


Fig. 10. Planar porosity analysis of the hybrid castings. Porous cores treated with a) no solution, b) 0.5% HF, c) 10% $H_3PO_4$ for 1.5 min, d) $H_3PO_4$ for 4 min

Table 5.
Planar porosity in orthogonal planes [%]

| Specimen | Plane XY | Plane YZ | Plane ZX |
|---|---|---|---|
| **N** | 12.0 | 9.2 | 9.7 |
| **F** | 18.1 | 26.5 | 28.9 |
| **P1** | 28.8 | 39.8 | 39.7 |
| **P4** | 35.2 | 46.7 | 47.0 |

The impact bending test was performed on four porous prismatic cores and two solid castings. The impact toughness, KC0, was calculated using relation (4). For the solid material, the ratio $m_P/m_S=1$. The foaming variant influenced the porosity of the prismatic foam cores. Porosity is the inverse of relative density, as determined from relation (2). For variants VP1 and VP2, the measured average porosity was 84.9 ± 1 %. For foaming variants VP3 and VP4, the average sample porosity was 78.6 ± 1.3 %.

The test results are recorded in Figure 11. The difference between the average energy absorbed by the foam cores and the average energy absorbed by the solid material of the same dimensions is 5.4 J, which represents a 42 % difference. The fundamental difference in density between the porous and solid materials, associated with a reduced cross-sectional area, resulted in significant differences in the impact toughness values. On average, the cores had 3.4 times higher impact toughness than the solid material. The highest KC0 value was found for the sample of variant VP4, which was foamed at pressures of 0.37 / 0.2 MPa and had a porosity of 80.2 %.

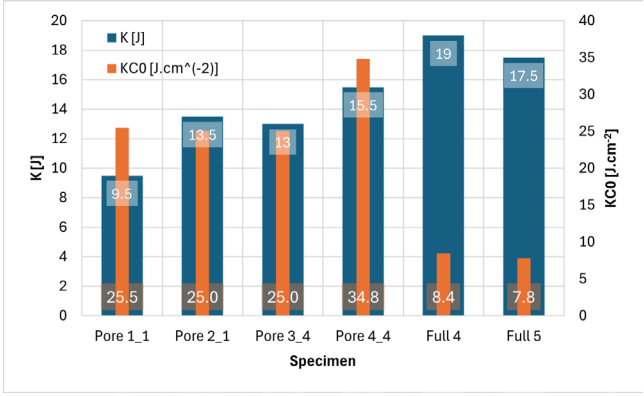


Fig. 11. Charpy impact test results

# 4. Conclusions

This study successfully established a methodological framework for testing and optimizing hybrid aluminum castings with porous cores. The findings demonstrate that both the initial foaming process and the subsequent surface treatment are critical control points that dictate the final mechanical performance.
The key conclusions are as follows:

1. **Controlled foaming pressure is essential for repeatability.** Uncontrolled foaming (V1) leads to high variability. Optimal and consistent compressive strength was achieved using starting pressures of 0.1–0.2 MPa with stabilizing pressures between 0.05 MPa and 0.101 MPa (variants V5 and V6).
2. **Surface treatment is the most critical factor for hybrid casting integrity.** Without proper preparation, the molten alloy infiltrates the core. Treatment with 10% $H_3PO_4$ was most effective, preventing infiltration and preserving the composite structure. This resulted in components with superior ductility and a compressive strength approximately three times higher than infiltrated castings.
3. **Porous cores offer high specific energy absorption.** The porous cores demonstrated an impact toughness (KC0) 3.4 times higher than solid specimens, confirming their suitability for lightweight applications where dynamic loading is a primary consideration. Also a significant observation from this study is that cores with a lower porosity of 78.6% (VP3 and VP4) demonstrated superior impact toughness compared to their more porous counterparts at 84.9% porosity (VP1 and VP2). The results, therefore, suggest that a cellular architecture with a higher relative density, characterized by thicker cell walls, offers a more optimized relationship between mass and energy absorption capacity for the specified geometry. This insight is critical for the micro-architectural design of foams tailored to specific dynamic loading applications.

In summary, this research confirms that by carefully controlling foaming parameters and applying an appropriate surface treatment ($H_3PO_4$), it is possible to manufacture high-performance hybrid castings that combine the strength of a solid shell with the lightweight, energy-absorbing properties of a metal foam core.

## Acknowledgements

The article was created as part of the grant agency projects: KEGA 029ŽU-4/2023, VEGA 1/0241/23. The authors thank the agency for support.


## References


[1] Liu, W., Peng, T., Kishita, Y., Umeda, Y., Tang, R., Tang, W. & Hu, L. (2021). Critical life cycle inventory for aluminum die casting: A lightweight-vehicle manufacturing enabling technology. *Applied Energy.* 304, 117814, 1-11. DOI: 10.1016/j.apenergy.2021.117814.

[2] Huang, Y., Tian, X., Li, W., He, S., Zhao, P., Hu, H., Jia, Q. & Luo, M. (2024). 3D printing of topologically optimized wing spar with continuous carbon fiber reinforced composites. *Composites Part B.* 272, 111166, 1-9. DOI: 10.1016/j.compositesb.2023.111166.

[3] Wang, B., Zhang, Z., Xu, G., Zeng, X., Hu, W. & Matsubae, K. (2023). Wrought and cast aluminum flows in China in the context of electric vehicle diffusion and automotive lightweighting. *Resources,* Conservation & *Recycling.* 191, 106877, 1-10. DOI: 10.1016/j.resconrec.2023.106877.

[4] Jasoliya, D., Shah, D.B. & Lakdawala, A.M. (2022). Topological optimization of wheel assembly components for all terrain vehicles. *Materials Today: Proceedings.* 59, 878-883. DOI: 10.1016/j.matpr.2022.01.221.

[5] Ali, M. A., Jahanzaib, M., Wasim, A., Hussain, S. & Anjum, N. A. (2018). Evaluating the effects of as-casted and aged overcasting of Al-Al joints. *The International Journal of Advanced Manufacturing Technology.* 96(1-4), 1377-1392. DOI: 10.1007/s00170-018-1682-x.

[6] Papis, K., Hallstedt, B., Löffler, J. & Uggowitzer, P. (2008). Interface formation in aluminium–aluminium compound casting. *Acta Materialia.* 56(13), 3036-3043. DOI: 10.1016/j.actamat.2008.02.042.

[7] Banhart, J. (2013). Light-Metal Foams—History of Innovation and Technological Challenges. *Advanced Engineering Materials.* 15(3) 82-111. DOI: 10.1002/adem.201200217.

[8] Lefebvre, L.-P., Banhart, J. & Dunand, D.C. (2008). Porous metals and metallic foams: Current status and recent developments. *Advanced Engineering Materials.* 10(9), 775-787. DOI: 10.1002/adem.200800241.

[9] Elzey, D.M. & Wadley, H.N.G. (2001). The limits of solid state foaming. *Acta Materialia.* 49(5) 849-859. DOI: 10.1016/S1359-6454(00)00395-5.

[10] Fu, W. & Li, Y. (2024). Fabrication, processing, properties, and applications of closed-cell aluminum foams: a review. *Materials*. 17(3), 560, 1-27. DOI: 10.3390/ma17030560.

[11] Matejka, M., Bolibruchová, D., Sýkorová, M. (2024). Effect of Ti addition on the hot-tearing susceptibility of the AlSi5Cu2Mg alloy. *Metals*. 14(6), 703, 1-20. https://doi.org/10.3390/met14060703.

[12] Ashby, M. (2000). *Metal foams: A Design Guide.* Elsevier: Burlington.

[13] Rajak, D. K., Gupta, M. (2020). *An Insight Into Metal Based Foams: Processing, Properties and Applications*. Singapore: Springer Nature.

[14] Gupta, N., Zeltmann, S. E., Doddamani, M. (2019). Testing of Foams. In Ch.-H. Hsueh (Eds.), *Handbook of Mechanics of Materials* (pp. 2083-2122). Singapore: Springer Verlag.

[15] Mudge, A. & Morsi, K. (2024). Fabrication of uniform and rounded closed-cell aluminum foams using novel foamable precursor particles (FPPs). *Metals.* 14(1), 120, 1-16. DOI: 10.3390/met14010120.